

## **Chapter 4**

### **Experimental Results of Erbium Doped MMI Waveguide Based on SOI Substrate by using Ion Implantation**

Through the completed theory and calculations of erbium-doped waveguide amplifier with integrated optical SOI waveguide devices are shown in Chapter 2, we try to fabricate and measure these erbium doped optical waveguide devices in this chapter. Owing to the excellent guided-wave characteristics of UNIBOND SOI substrates exhibited in waveguide devices, we focus on our attentions on the SOI waveguide devices based on UNIBOND SOI wafers. The substance of Chapter 4 is organized as follows: The basic semiconductor processes are discussed in Section 4-1. Section 4-2 introduces the technique and operating steps of ion implantation. The experiment processes and results of integrated optical Multimode interference waveguide based on UNIBOND SOI wafer which doped erbium are presented in Section 4-3. We also give the conclusions and discussions of our erbium doped SOI optical devices in section 4-4.

## **4-1 Introduction of UNIBOND SOI Wafer with “*Smart-Cut Process*”**

The based substrates we chose in fabricating integrated optical waveguide devices are UNIBOND SOI wafers. In this section, the technique of UNIBOND SOI materials with “smart-cut process” is described and essentially comprised as following four steps in Fig. 4-1:

Step 1: Using ion implantation to implant the ions of hydrogen (dose =  $2 \times 10^{16} \sim 1 \times 10^{18} \text{ cm}^{-2}$ ) in a silicon wafer: This wafer is preferably capped before implantation with a dielectric layer, e.q. thermally grown  $\text{SiO}_2$ . This dielectric layer becomes the buried oxide of the SOI structure.

Step 2: Wafer A is hydrophilic bonded at room temperature of wafer A to a wafer B: Wafer B is either bare or capped. Both wafers are cleaned using a modified RCA process before bonding. Wafer B is very important in the “smart-cut process” because it is a stiffener and provides the bulk silicon under the buried oxide in the SOI structure.

Step 3: Two-phase heat treatment to this two bonded wafers: During the first treatment phase ( $400^\circ\text{C} \sim 600^\circ\text{C}$ ), the implanted wafer A splits into two parts: a thin layer of monocrystalline silicon remaining bonded wafer B and the rest of wafer A, which can be recycled for use as another wafer B. The second high temperature treatment phase ( $> 1000^\circ\text{C}$ ) aims to strengthen the chemical bonds.

Step 4: Fine polishing: After splitting, the layer exhibits a micro-roughness which makes chemo-mechanical polishing of the surface necessary.

After describing the four steps of the “smart-cut process”, we summarize

the advantages of this technique as following terms:

(1) Thickness uniformity: The silicon upper layer of the SOI structure is obtained by separation at the mean ion penetration depth. The thickness is only related to the ion energy ( $\sim 8\text{nm/keV}$  in silicon) with no evidence of dose effect. As the implantation profiles of hydrogen ions are very sharp and the ion energy is accurately and easily controlled, the layer thickness after splitting is inherently homogeneous (dispersion  $< 4\text{ nm}$ ). The achievable thickness dispersion after polishing is close to  $8\text{ nm}$  for an average thickness of  $200\text{ nm}$  on a  $10\text{ cm}$  wafer.

(2) Crystalline quality: The use of medium implantation dose and light ions minimizes atomic displacement, giving rise to high crystalline quality SOI layers.

(3) Electrical properties: ULSI electronic devices with ultrathin gate oxides ( $40\text{\AA}$ ) have been realized on “smart-cut process” wafers. The breakdown intrinsic field measured on  $0.03\text{mm}^2$  capacitors is  $16\sim 17\text{MV/cm}$  which is comparable to results of the best bulk silicon material.

The “smart-cut process” appears highly suitable for making high quality SOI wafers with the great advantages of intrinsic low defect density and thickness homogeneity. All the basic steps involved can be performed on standard microelectronics facility equipment (ion implanters, furnaces, wet bench, polishing machines). No wafers are wasted in the grinding and thinning operations; a single bulk silicon wafer is required to achieve an SOI wafer.

## 4-2 Introduction of Ion Implantation

The appearance of high density chips makes the smaller size of fabrication. And the alternate distance of each other of the circuit part is also smaller. Using method of thermal diffusion is limited while making a more progressive chip which includes five kinds of problem:

1. Diffusion horizontally.
2. It is difficult to produce the ultra shallow junction.
3. Doping cannot be controlled well.
4. Pollution on the surface
5. Dislocation. We can overcome the restriction of spread and offer other advantages by ion implantation.

Ion implantation is a process in which energetic, charged atoms or molecules are directly introduced into a substrate. It can applied to source/Drain formation, channel stopper, bipolar formation, photoresist hardening, silicon on insulator using oxygen implant, etc.

It has some advantages:

1. Better concentration control
2. Less lateral distribution
3. More pure dopant available
4. Single implantor for various implant species
5. Better uniformity across large wafer
6. A variety of masking materials can be used
7. Low temperature process
8. Less contamination

But it also has problems and limitations:

1. Ion implantation will cause damage to the Si substrate so the wafer

need thermal processes to anneal these damages.

2. Ion implantation is a complex machines so it need conscientiously operated and maintained by well trained personnel.
3. It contains many hazards, such as hazardous chemicals, high voltage, and radiation and we need to follow safety procedures strictly.

We must also consider the case of channeling effect: if the ion beam enters the silicon lattice along a crystallographic direction, the beam travels a much greater distance than in an amorphous solid by axial “channeling” between lattice planes, producing an additional distribution.

Ion implantation will not cause and spread horizontally and can operate close room temperature. The dopant can be implanted below the surface of the wafer and we can decide the location, amounts and the distribution of the dopant in the device via ion implantation. At the same time, photoresistance and a thin metal layer can be used for disconnection, like silica. Because it has the above advantages, ion implantation can be used for doping into the most progressive wafers, and the diffusion still used for low integrated devices.

In this section, we will show the physical meaning of ion implantation and the following is the procedure of ion implantation and is also shown in Fig. 4-2.

**Ion Source:** the ion source is a cavity. We generate ions to be implanted.

**Extraction/Acceleration:** ions are given a high voltage. Simultaneously, the ion are attracted toward the ground electrode and accelerated through the aperture.

**Mass analyzer:** when ion beams pass through the mass analyzer, due to different particles having different atomic weight, we produce a magnetic field to select the ion species of interest according to their mass and reject all others. According to this equation, we can select the ion which we want to pass through the mass analyzer. We can use the effect of a magnet on a charged particle and bending radius formula:

$$Mv^2 / r = BqeV \quad (3-1)$$

**Extraction energy**  $E = qeV = mv^2 / 2 \quad (3-2)$

**So**  $v = (2E / m)^{\frac{1}{2}} = (2qev / m)^{\frac{1}{2}}$

$$\begin{aligned} r &= mv / (Bqe) = (2mE)^{\frac{1}{2}} / (Bqe) \\ &= (2mv / qe)^{\frac{1}{2}} / B \end{aligned} \quad (3-3)$$

their radius of gyration will be different so the ions can be separated by means of a magnetic field which we calculate and show in Fig. 4-3.

**Acceleration System:** ions pass through the acceleration tube. It can help increase speed of the ions due to the attraction between electrons and positive ions. We can accelerate the ion to increase energy and focus the ion beam to a particle size and shape. If the acceleration voltage is bigger, the velocity will increase and we will have enough momentum to implant ions into the wafer.

**Q-Lens:** Since the ion beams are also constructed by positive ions, when the ion beam leaves the acceleration tube, the ions will reject each other,

so we use a Q-lens to focus the ion beam and distribute the ions uniformly over the target.

**Electrostatic Deflector:** The ions pass through the electrostatic deflector. Because there are remain some gas molecule, such particles will collide with the ion beam and become neutral atoms, so we use the electrostatic deflector to change the direction of the ion beam, and the neutral atom will continue forward as shown in Fig. 4-4. The ion beam is then implanted into the SOI waveguide on target.

**Dose Control:**

In this procedure, we use the Faraday's theory of operation: electrons used=ions neutralized. So the beam current to dose conversion is:

$$1\mu A = 1\mu C / \text{sec}$$

$$1\mu C = 6.3 \times 10^{12} \text{ ions} / \text{sec}$$

In the following sections, we will describe our structure of MMI as Erbium doped waveguide amplifier which implanted  $\text{Er}^{3+}$  by means of ion implantation.

## 4-3 Experimental Results of Erbium Doped MMI Waveguide

### Amplifier

According to the previous discussions of fabricated techniques of UNIOND SOI wafers with “smart-cut process” and ion implantation, we have fabricated a erbium doped optical multimode interference waveguide (MMI) based on SOI substrate. We use ion implantation to dope the  $\text{Er}^{3+}$  into our device. Our implanted energy is 100KeV. In this sample, the dose is  $3 \times 10^{14}/\text{cm}^2$  and range from just under the silicon surface to a depth of  $0.07 \mu\text{m}$  as shown in Fig. 4-5. Fig. 4-6 shows the close view of the erbium doped 2x2 MMI input port and output port. The cross section of single mode rib waveguide based on SOI wafer by scanning electron microscope (SEM) is shown in Fig. 4-7. The width of rib waveguide  $W$ , the height of slab waveguide  $h$  and the total rib height  $H$  is  $4 \mu\text{m}$ ,  $2 \mu\text{m}$ , and  $2.5 \mu\text{m}$ , respectively.

We try to measure the gain of the wafer by two methods. The initial experimental setups for measuring the output beam from the output port of rib waveguide are shown in Fig. 4-8 and the second are shown in Fig. 4-9. The first one we use collimator to align the input signal to MMI and the second we use single mode fiber. The first type of our experimental setup: our light source is the tunable wavelength laser with  $\lambda=1550\text{nm}$  and the pump source is a 980nm pump laser which pass through the 2 x 2 WDM fiber coupler connecting to collimator and objective lens to the experiment stage and the optical spectrum analyzer (OSA). The second type of experimental setup: we use single mode fiber to replace the



collimator and objective lens to aim our device and passing through the experiment stage and the optical spectrum analyzer (OSA). The UNIBOND SOI waveguide samples are set on the rotation stage, translation stage and the x, y, z tilted stage, respectively. They can be rotated, positioned and adjusted, until the mode pattern is detected by the infrared (IR) CCD camera. The IR camera then connects to the computer and image capture card. We set the input signal from tunable wavelength laser through input single mode fiber which established on rotated, positioned, and adjusted using the rotation stage for decreasing coupling loss. We put the MMI wafer on the stage, then we can find the same focal length between our sample and input fiber by microscope to decrease the insertion loss and coupling loss. The picture of two kinds of experiment frames with measuring 2 x 2 Multimode Interference (MMI) is shown in Fig. 4-10 and Fig. 4-11. According to our experimental flow path with a light source wavelength of 1550nm and pump source wavelength of 980nm, the output near-field images and the output mode pattern of one output channel of MMI are recorded and shown in Fig. 4-12. From Fig. 4-12, we change the power from 16mw (50mA) to 78mW (100mA) of 980nm pump laser, we can find the different pump power increase the output power and shown in Fig. 4-13 ~ 4-18. The saturation pump power is about 78mW and Maximum signal enhancement is about 0.56dB/cm. The relationship between pump power and output power of MMI is shown in Fig. 4-19.

## 4-4 Summary

The SOI material technology based on wafer bonding and ion implantation is described in this chapter. The SOI wafers fabricated with “*smart-cut process*” appears highly suitable for making high quality SOI wafers with great advantages of intrinsic low defect density and thickness homogeneity. We implanted  $\text{Er}^{3+}$  into the waveguide as a gain medium and controlled the concentration and depth precisely by ion implantation precisely. In this chapter, the guide-wave propagated along the SOI rib waveguide device can be confined and the output light mode pattern and net gain has been presented obviously. The experimental equipment also plays an important role in the performance of our device. However, few defects were presented in the experimental results. The blemish phenomenon of experimental results of the erbium doped SOI waveguide devices can be summarized as in following:

1. Our experimental setup needs more stable condition to keep the precise mode pattern and output power, focusing the diameter of single mode fiber, while matching the width of rib waveguide in a stable surrounding is very difficult.
2. Although the vertical side of SOI waveguide device has been polished, it is not very standing  $\cong 90^\circ$ .
3. The imperfectible experimental environment.  
(including the experimental instruments, dust in the air, etc.)
4. The gain limiting factor we must consider: Depth of  $\text{Er}^{3+}$  in our device, the dose of  $\text{Er}^{3+}$ , waveguide losses, ESA, Mode overlap, pump absorption...etc.

Although the few deviations presented in our designed erbium doped optical SOI waveguide devices, the characteristics of such erbium doped SOI waveguide devices still show promising results for applying to photonic integrated devices in future optical systems applications.

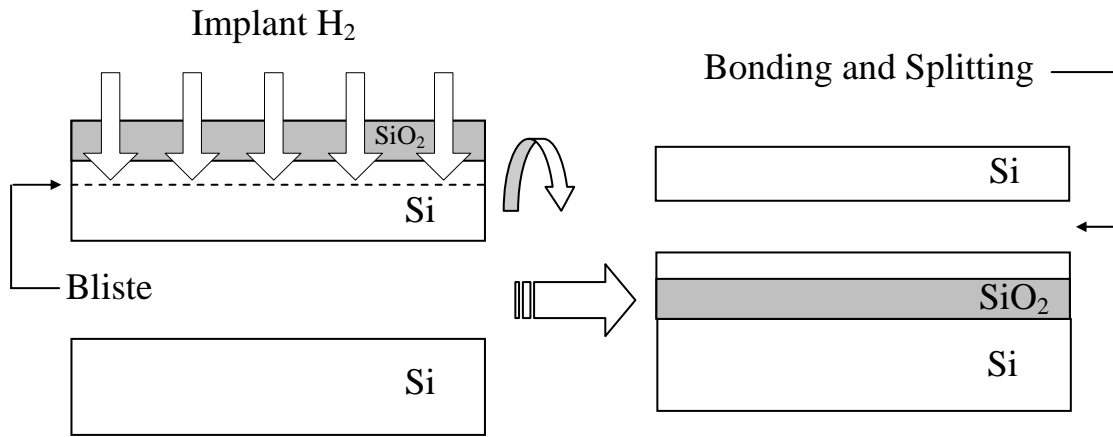


Fig. 4-1 Method of UNIBOND SOI

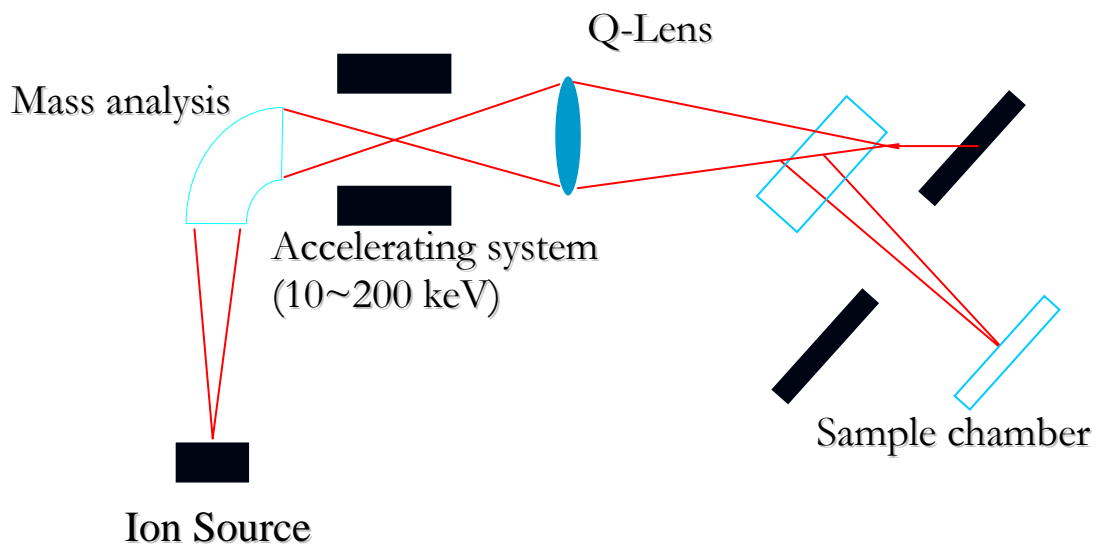


Fig. 4-2 Procedure of ion implantation

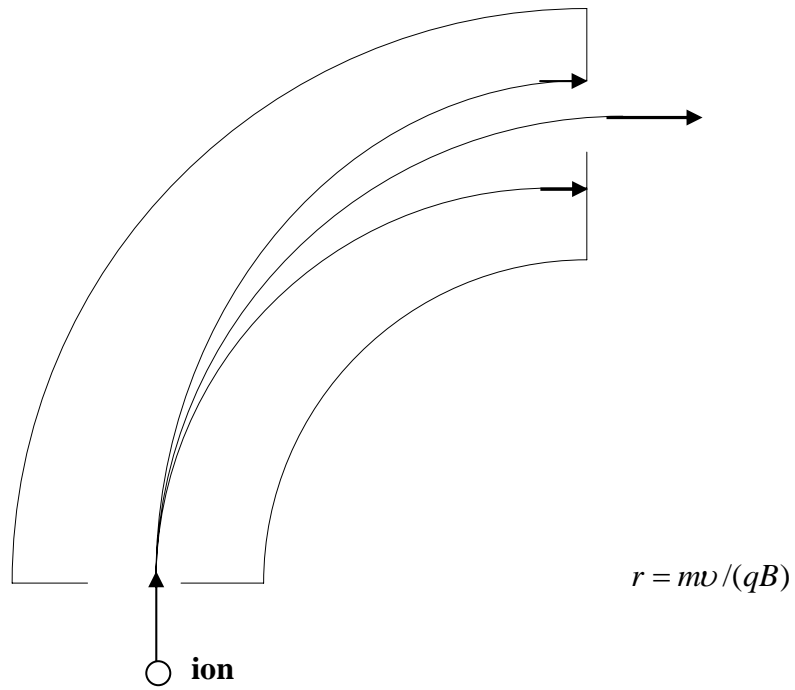


Fig. 4-3 Procedure of mass analyzer

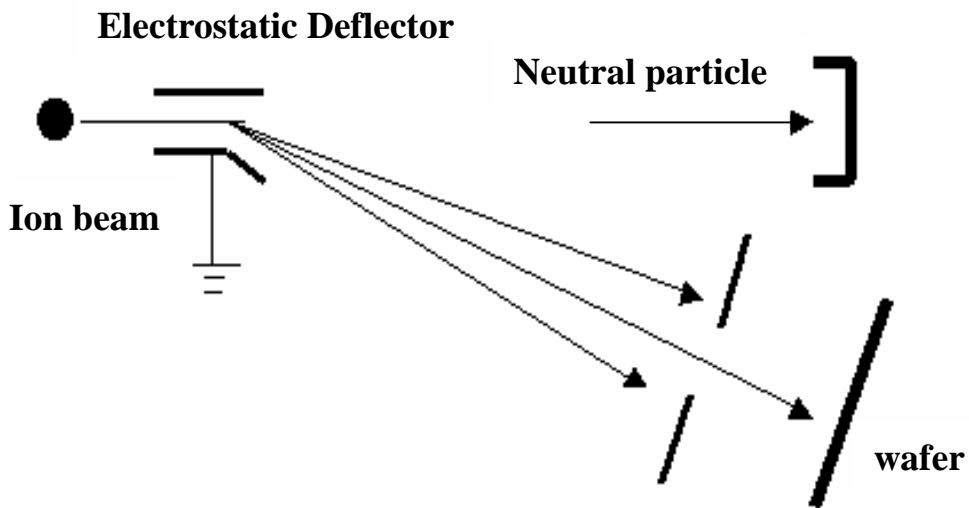


Fig. 4-4 Procedure of Electrostatic Deflector

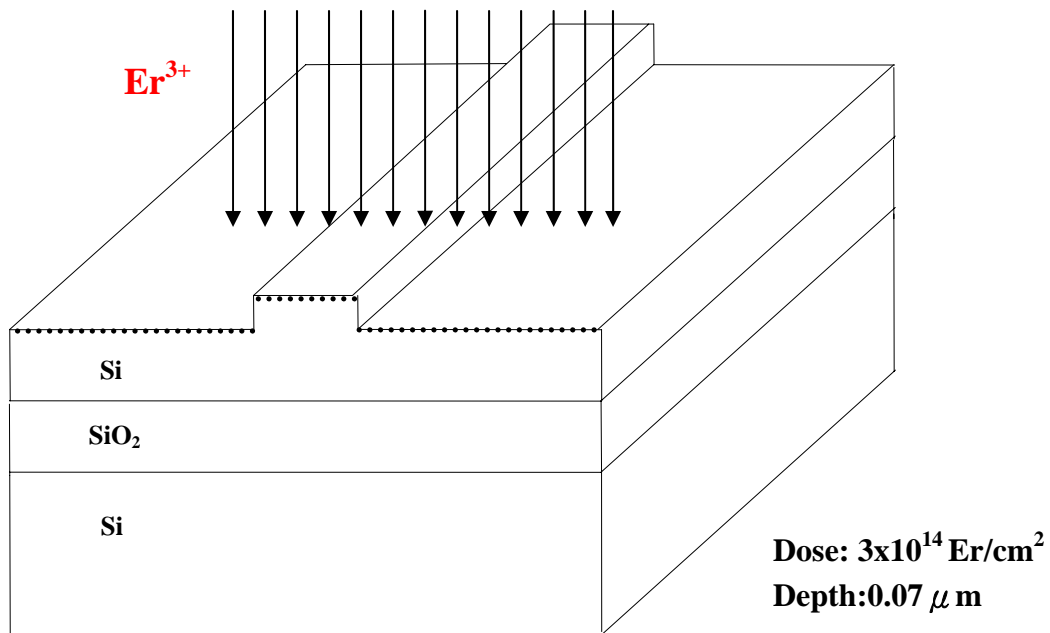


Fig. 4-5 Picture of the dose and the depth of  $\text{Er}^{3+}$  under the Silicon surface

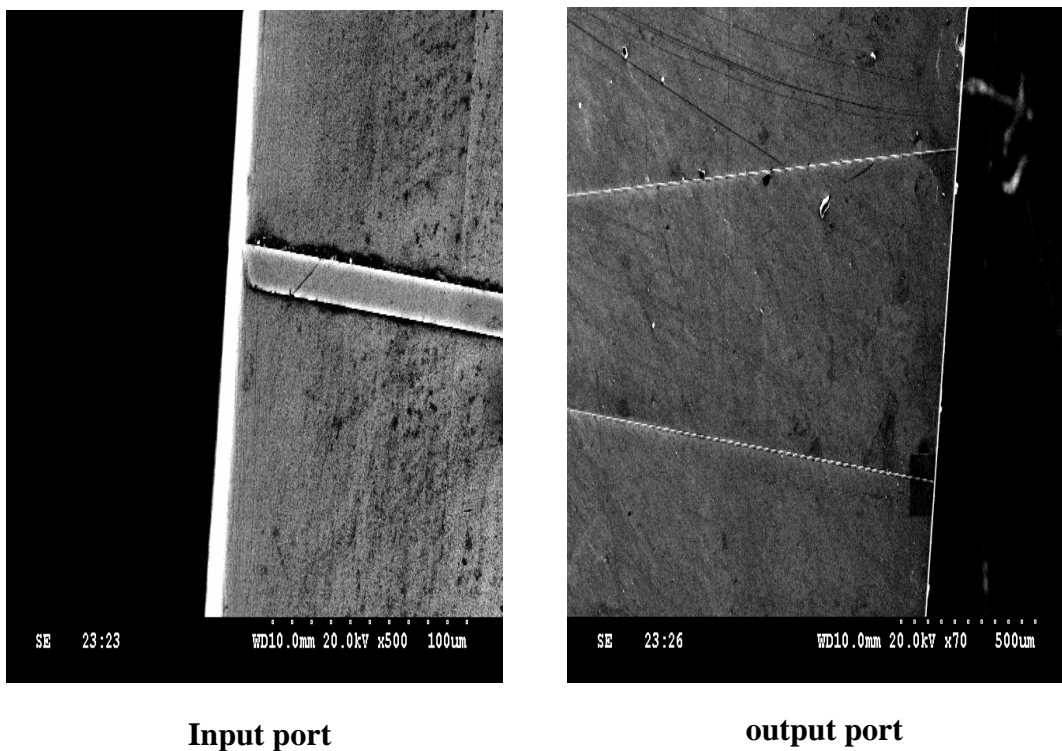


Fig. 4-6 Input port and output port of  $\text{Er}^{3+}$  MMI by SEM

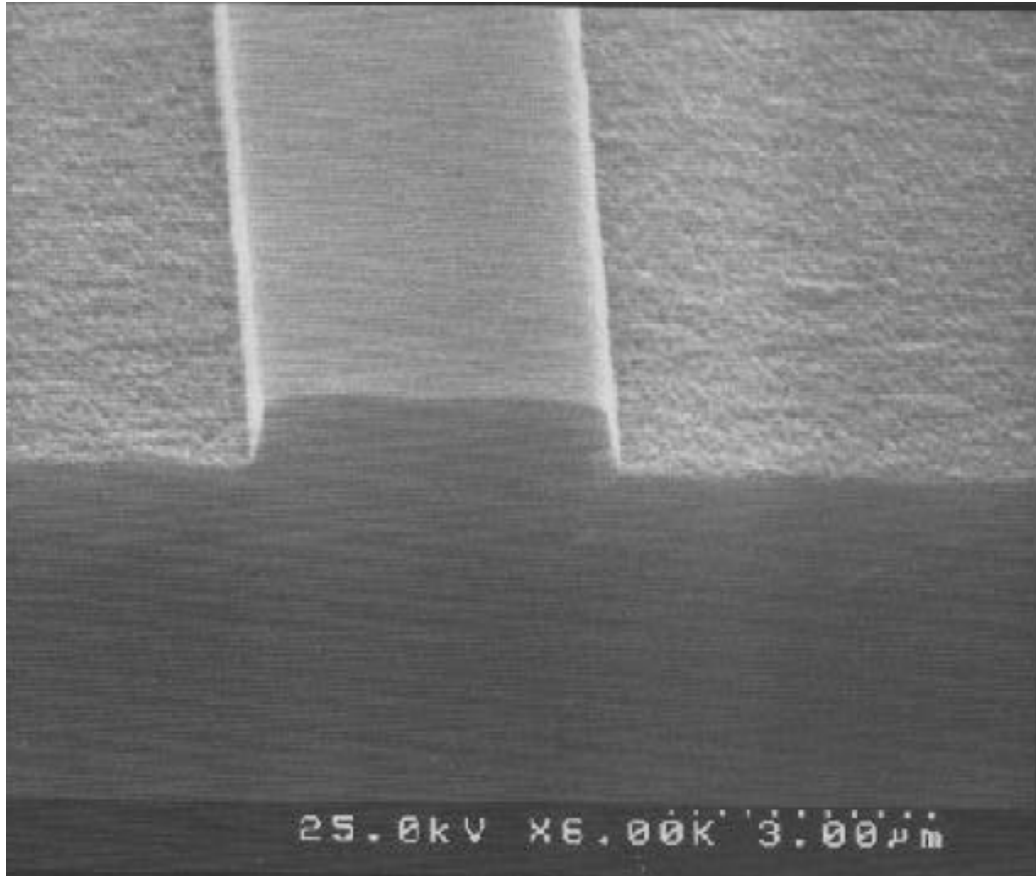


Fig. 4-7 Cross section of the SOI single mode rib waveguide by SEM

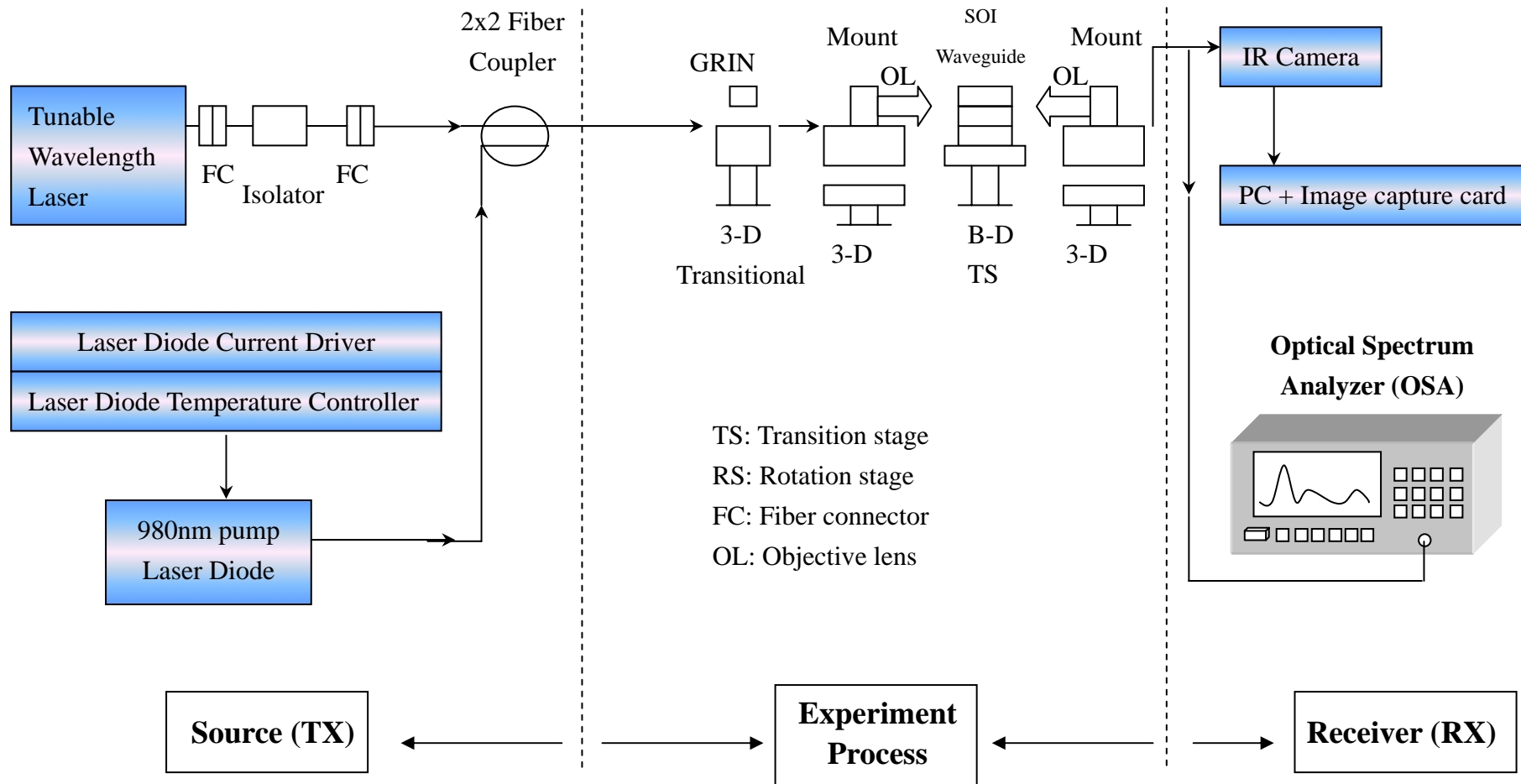


Fig.4-8 First experimental setups for measuring the output beam from the one channel of 2 output ports of MMI with source wavelength = 1550nm



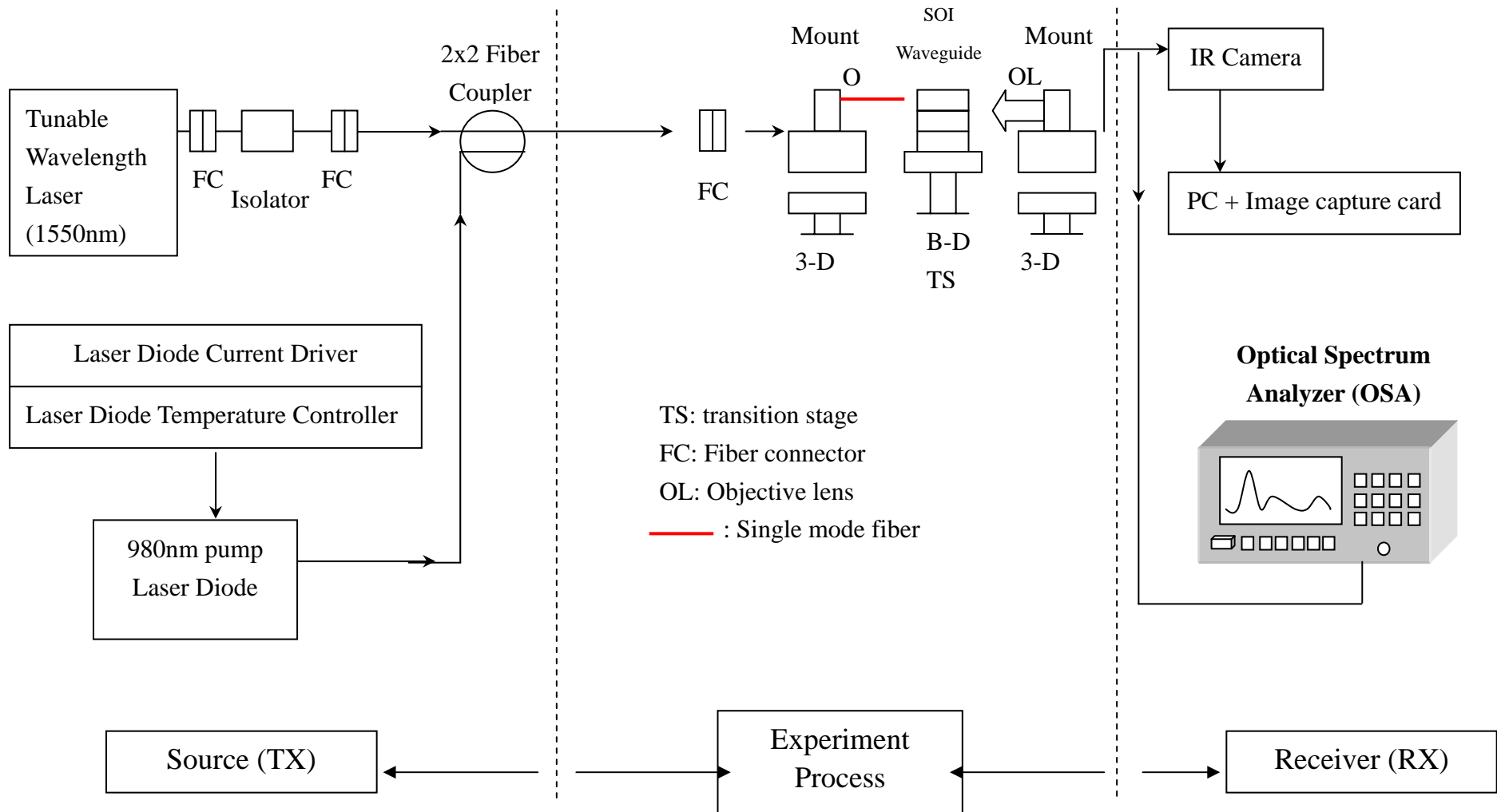


Fig.4-9 Second experimental setups for measuring the output beam from the one channel of 2 output ports of MMI with source wavelength = 1550nm

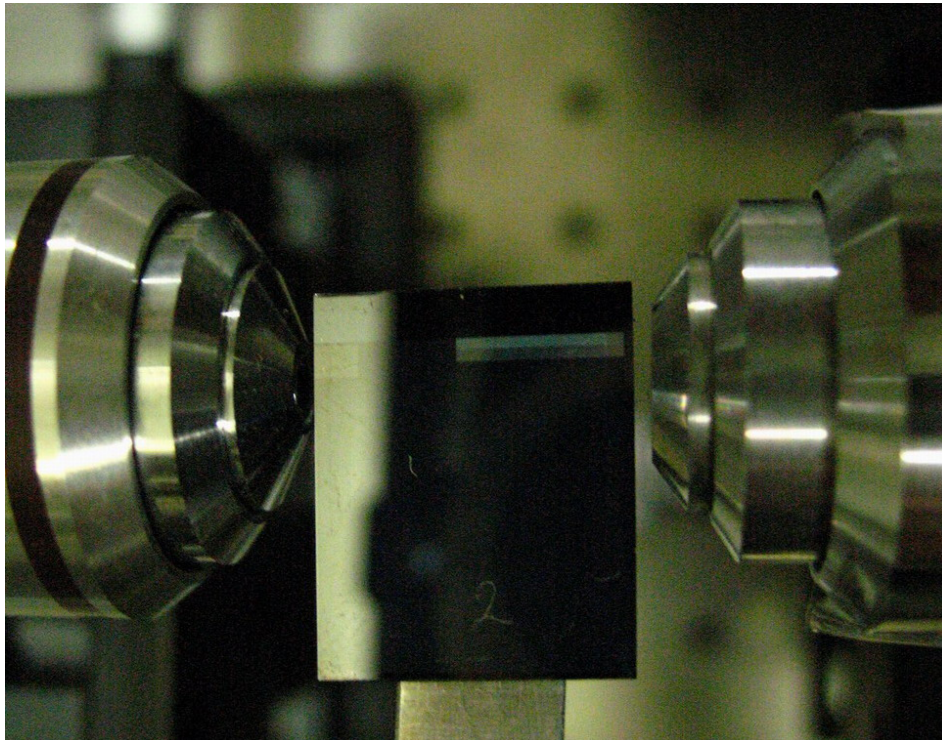


Fig. 4-10 Picture of first experiment frame with measuring optical 2x2 MMI waveguide

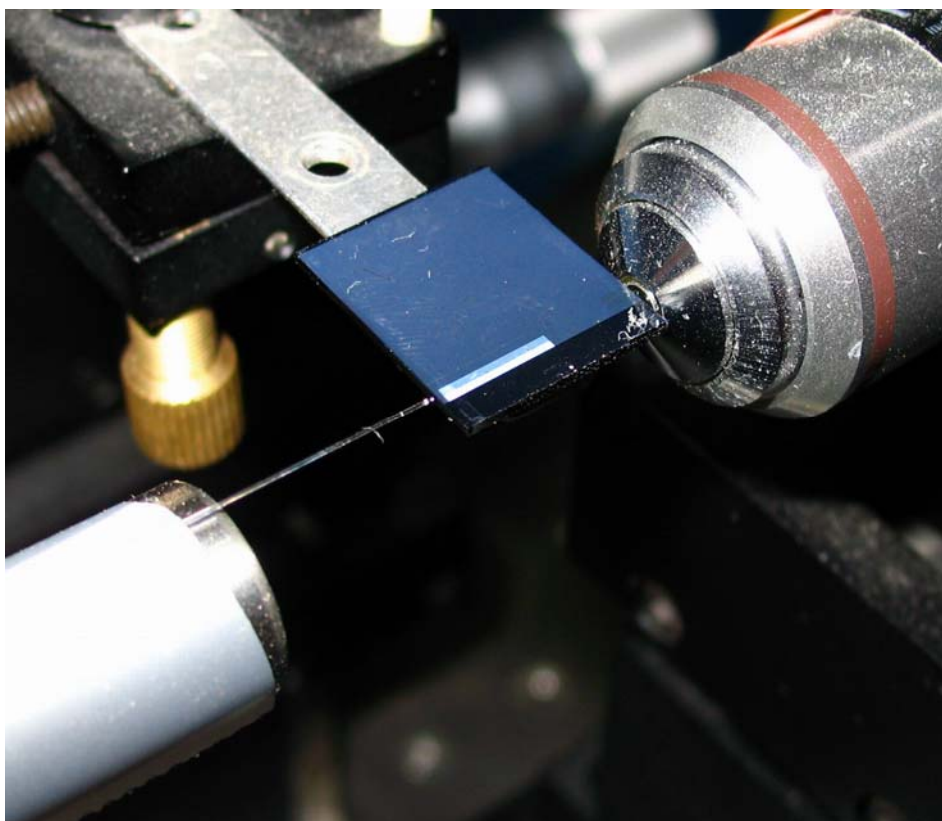


Fig. 4-11 Picture of second experiment frame with measuring optical 2x2 MMI waveguide

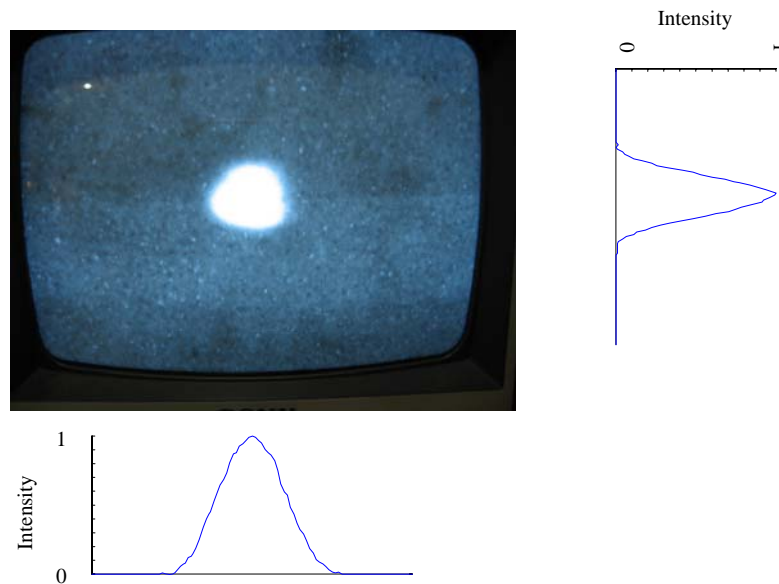


Fig. 4-12 Output mode pattern of one channel of 2x2 MMI

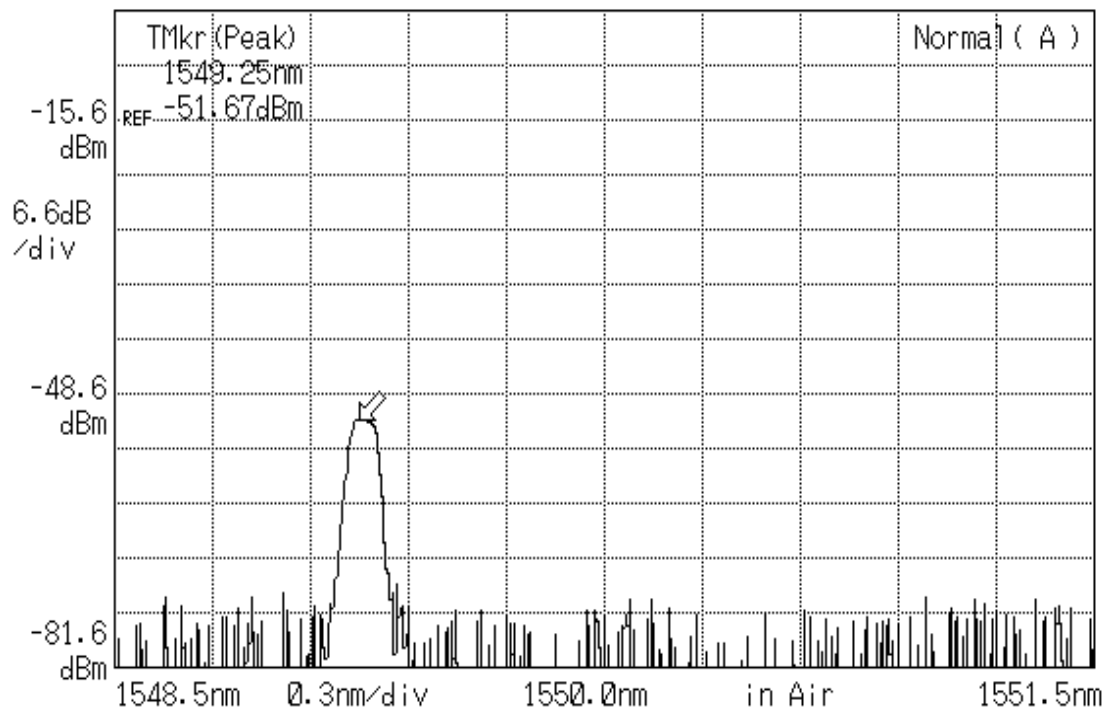


Fig. 4-13 Output power of MMI with 980nm pump laser optical power: 0mW

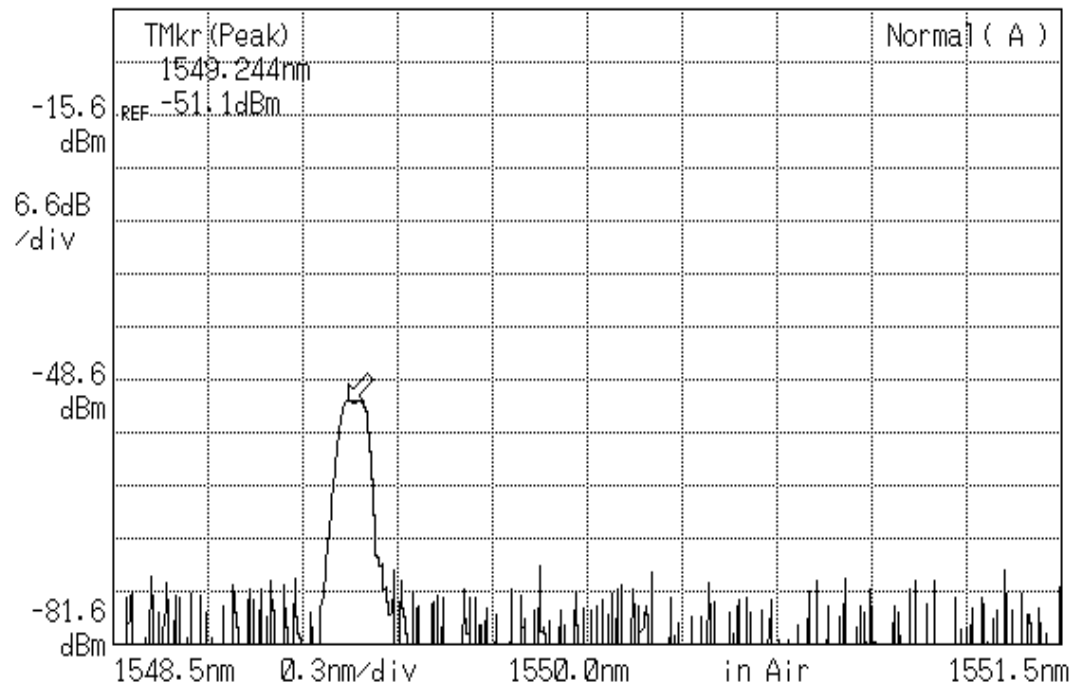


Fig. 4-14 Output power of MMI with 980nm pump laser optical power: 16mW

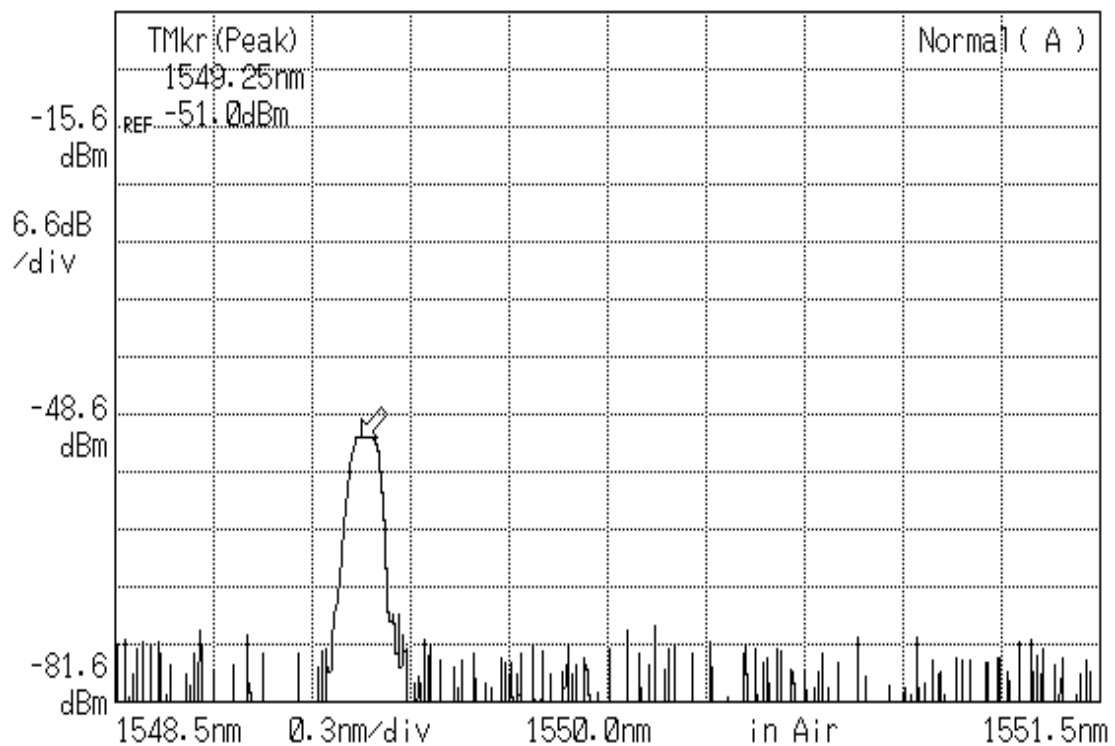


Fig. 4-15 Output power of MMI with 980nm pump laser optical power: 21mW

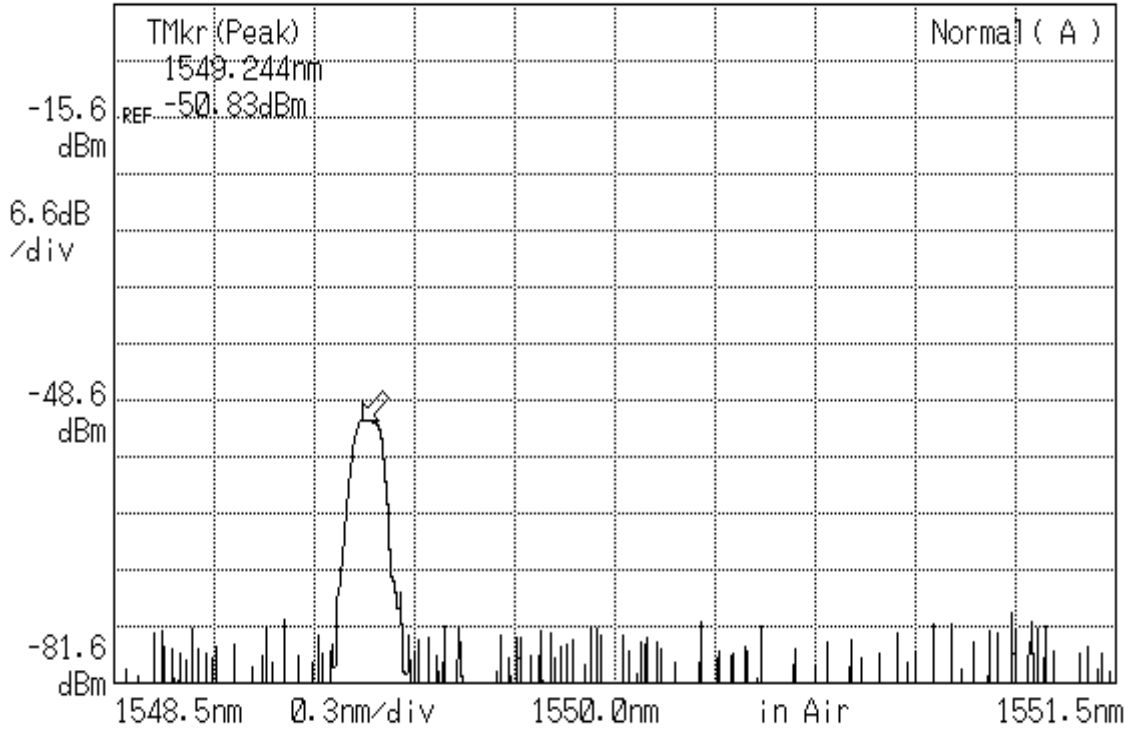


Fig. 4-16 Output power of MMI with 980nm pump laser optical power: 28mW

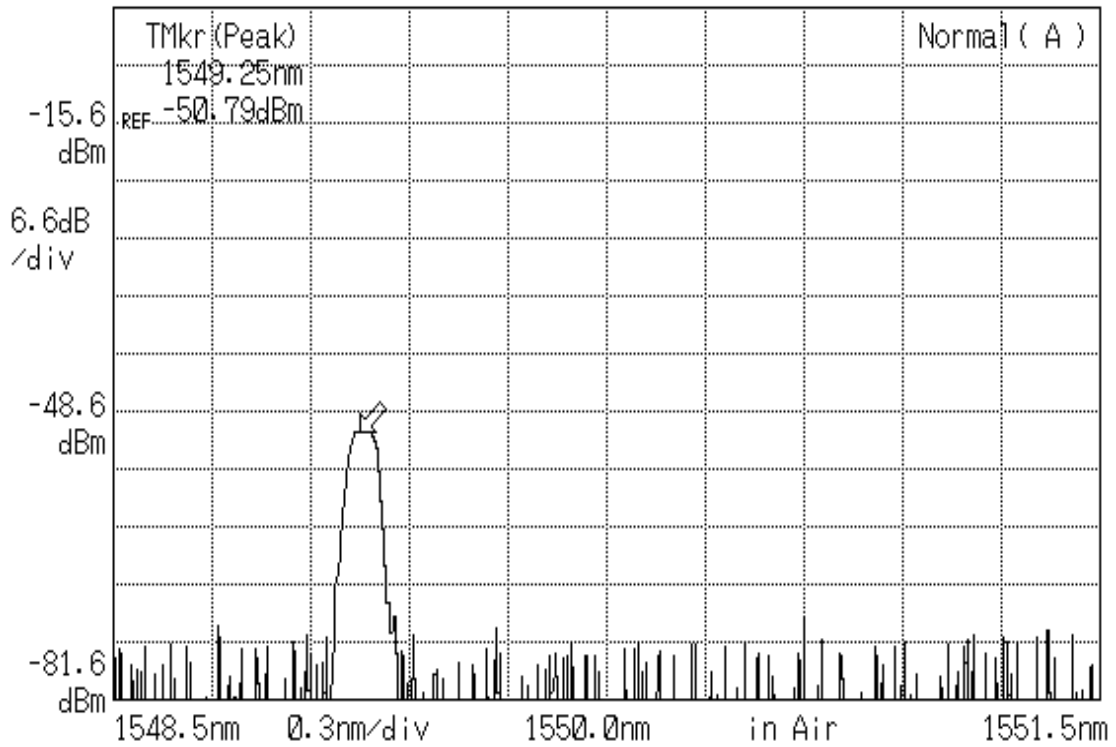


Fig. 4-17 Output power of MMI with 980nm pump laser optical power: 34mW

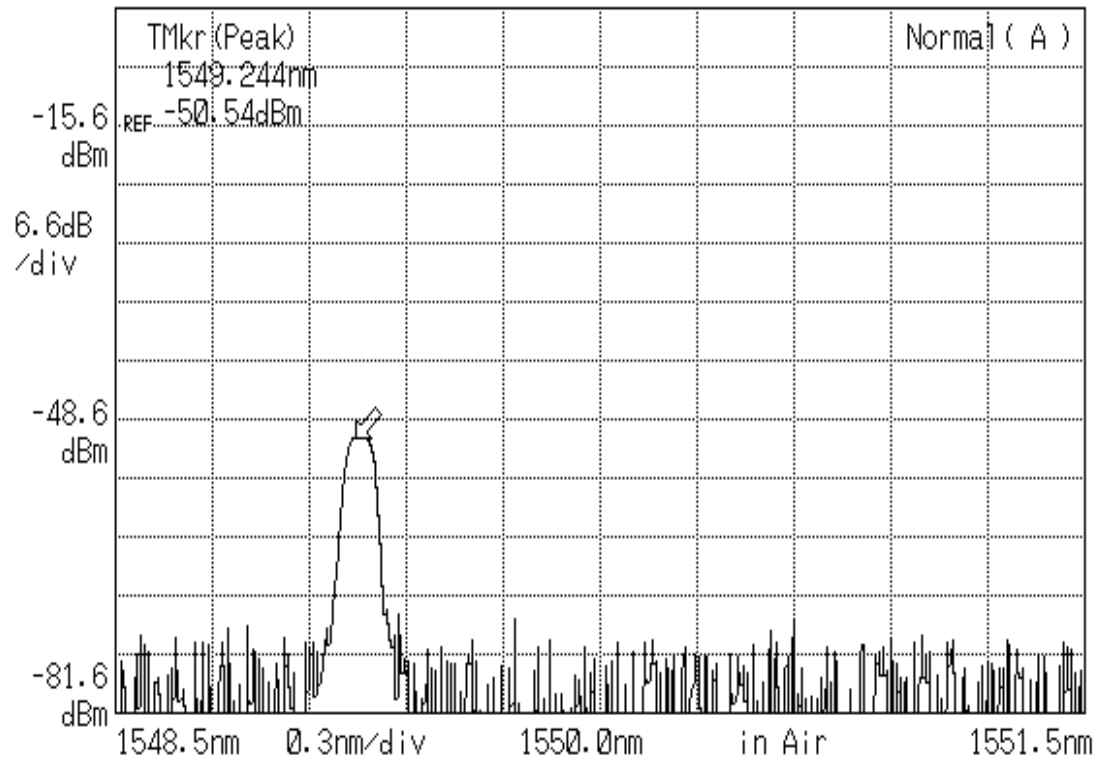


Fig. 4-18 Output power of MMI with 980nm pump laser optical power: 78mW

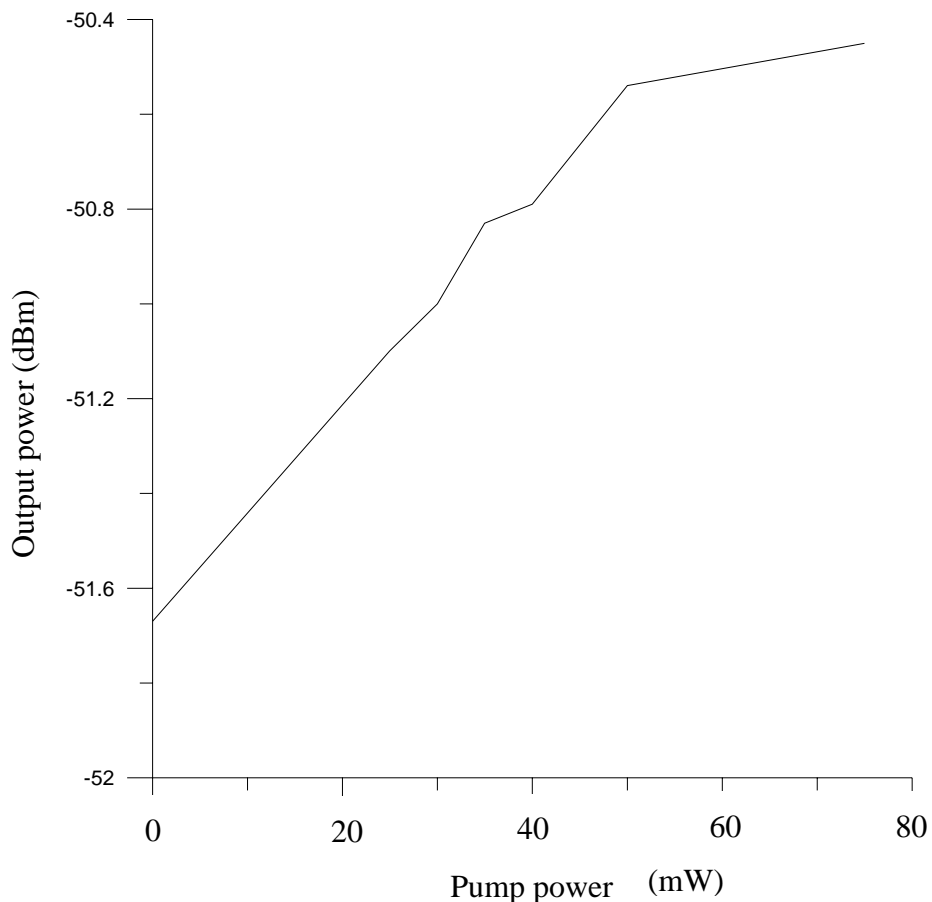


Fig. 4-19 Relationship between pump power and output power at 1549nm